Optics and Spectroscopy, 2025, Vol. 133, No. 3

09

Dynamic microcavities and time-dependent media in collisions of unipolar attosecond pulses of different shapes

© R.M. Arkhipov[1], M.V. Arkhipov[1], O.O. Diachkova[1,2], N.N. Rosanov[1]

[1] Ioffe Institute, St. Petersburg, Russia
[2] St. Petersburg State University, Saint-Petersburg, Russia

E-mail: arkhipovrostislav@gmail.com, mikhail.v.arkhipov@gmail.com, o.o.dyachkova@gmail.com, nnrosanov@mail.ru

Received February 19, 2024
Revised February 19, 2024
Accepted February 28, 2024

Optics of time-varying media has been actively developing in recent decades due to new possibilities for controlling the properties of light in space and time using such media. The advent of extremely short light pulses, up to unipolar half-cycle pulses, opens up new possibilities for ultrafast control of the properties of a medium in space and time on times of the order of half the field period, which are inaccessible for conventional multi-cycle pulses. In this paper, we numerically study the dynamics of Bragg microresonators in a three-level medium whose properties vary in space and time. This occurs when unipolar light pulses of different time shapes, Gaussian and rectangular, collide in it, having a small amplitude at which the medium is slightly excited and does not return back to the ground state after the passage of the pulses. We discuss broader possibilities for controlling the properties of a medium in space and time by using half-cycle pulses of different time shapes as a result of symmetric and asymmetric collisions of pulses in the medium.

Keywords: time-dependent media, optical microresonators, half-cycle pulses, attosecond pulses, atomic coherence, coherent effects.

DOI: 10.61011/EOS.2025.03.61167.7626-24

Introduction

Optical microresonators with a high *Q*-factor have been extensively studied in optics in recent decades [1–3]. Interest in them stems from their numerous potential applications, such as optical frequency comb generation [4–5], compact laser source development [6], strong-coupling regime studies of exciton-polariton dynamics [7], biological sensors [8], and other applications. Such microresonators can be made, for example, from quartz nanoparticles having whispering gallery modes or photonic crystals [1–8]. But the parameters of such structures are embedded in them during manufacturing and cannot be quickly changed. This imposes a number of limitations on the use of such structures in the tasks of modern ultrafast optics.

To date, media whose optical properties (refractive index) can be changed rapidly in time (*time varying medium*) [9] or simultaneously in space and time (spatiotemporal photonic crystals) are actively studied [10]. These artificial media are of interest in optics, in the problems of controlling the propagation of light in both space and time. On the other hand, a number of interesting phenomena, such as temporal reflection and temporal refraction, parametric amplification, and more, can occur in such media when the refractive index changes rapidly, see review [9].

But changing the properties of the medium in space and time is a complex practical problem. Currently, multi-cycle femtosecond pulses of laser radiation have been used for this purpose [11]. With the advent of attosecond pulses, it became possible to study and control the motion of electrons in matter at times comparable to the period of the electron's turnover along the Bohr orbit in the atom (hundreds of attoseconds) [12].

But the studying and controlling the properties of substances at shorter times requires extremely short half-cycle pulses consisting of a half-wave field. Such pulses with nonzero electrical area,

$$S_E = \int E(r,t)dt, \tag{1}$$

($E(r,t)$ is field strength at a given point of space, t is the time) [13] are promising for ultrafast control of the properties of quantum systems and ultrafast switching of the state of matter in much faster times than conventional multicycle pulses. The results of recent studies in the production and application of such pulses are summarized in the reviews [13,14] and the monograph [15].

The physics of the interaction of such pulses with matter is quite unusual; we have to abandon a number of typical theories and concepts that are valid for multicycle pulses [13–15]. Under these conditions, many new and unusual phenomena occur that seem impossible with multicycle pulses.

It turned out that the collision of half-cycle pulses in matter can create high-voltage dynamic microresonators (DM) at each resonance transition of the medium [16–18]. The population difference of atomic transitions remains nearly constant within the pulse overlap region. It either changes by a jump to a different value outside this region. Either a Bragg lattice of atomic populations is created in this region. The shape of DMs can be controlled by multiple collisions between pulses, indicating the dynamical nature of such structures. An overview of recent research results in this area can be found in Ref. [19].

In early studies [16–19] such structures were studied in case of a collision of unipolar pulses of the same shape — Gaussian or rectangular. The shape of the induced structures obviously depends on the shape of the pulses. For application of such structures it is important to study their properties depending on the parameters of external excitation and other factors. Analytical approaches [18] to describe DM are developed on the basis of rough approximations and have a limited area of applicability. The full picture can only be revealed by numerical modeling.

We study in this paper the behavior of DM (doublet molecules) during multiple collisions of half-cycle pulses with different profiles (rectangular and Gaussian) in a medium, based on numerical solutions of the density matrix equations for a three-level system coupled with the wave equation. We consider the case of small weak excitation of the medium, when the impact of pulses leads to an insignificant emptying of the ground state of the medium (the regime of self-induced transparency, when the medium returns to the ground state after pulses, is not considered in this paper).

Calculated model and calculation results

The numerical model is based on a system of equations for off-diagonal elements of the density matrix (ρ_{21}, ρ_{32}, ρ_{31}), diagonal elements (ρ_{11}, ρ_{22}, ρ_{33}), representing the population densities of the 1st, 2nd and 3rd medium states (corresponding to atomic level populations), medium polarization $P(z,t)$, wave equation for the electric field strength [20]:

$$\frac{\partial}{\partial t}\rho_{21} = -\frac{\rho_{21}}{T_{21}} - i\omega_{12}\rho_{21} - i\,\frac{d_{12}}{\hbar}\,E(\rho_{22}-\rho_{11}) - i\,\frac{d_{13}}{\hbar}\,E\rho_{23} + i\,\frac{d_{23}}{\hbar}\,E\rho_{31}, \quad (2)$$

$$\frac{\partial}{\partial t}\rho_{32} = -\,i\omega_{32}\rho_{32} - i\,\frac{d_{23}}{\hbar}\,E(\rho_{33}-\rho_{22}) - i\,\frac{d_{12}}{\hbar}\,E\rho_{31} + i\,\frac{d_{13}}{\hbar}\,E\rho_{21}, \quad (3)$$

$$\frac{\partial}{\partial t}\rho_{31} = -\,i\omega_{31}\rho_{31} - i\,\frac{d_{13}}{\hbar}\,E(\rho_{33}-\rho_{11}) - i\,\frac{d_{12}}{\hbar}\,E\rho_{32} + i\,\frac{d_{23}}{\hbar}\,E\rho_{21}, \quad (4)$$

$$\frac{\partial}{\partial t}\rho_{11} = i\,\frac{d_{12}}{\hbar}\,E(\rho_{21}-\rho_{21}^{*}) - i\,\frac{d_{13}}{\hbar}\,E(\rho_{13}-\rho_{13}^{*}), \quad (5)$$

$$\frac{\partial}{\partial t}\rho_{22} = -i\,\frac{d_{12}}{\hbar}\,E(\rho_{21}-\rho_{21}^{*}) - i\,\frac{d_{23}}{\hbar}\,E(\rho_{23}-\rho_{23}^{*}), \quad (6)$$

$$\frac{\partial}{\partial t}\rho_{33} = -\frac{\rho_{33}}{T_{33}} + i\,\frac{d_{13}}{\hbar}\,E(\rho_{13}-\rho_{13}^{*}) + i\,\frac{d_{23}}{\hbar}\,E(\rho_{23}-\rho_{23}^{*}), \quad (7)$$

$$P(z,t) = 2N_0 d_{12}\mathrm{Re}\rho_{12}(z,t) + 2N_0 d_{13}\mathrm{Re}\rho_{13}(z,t) + 2N_0 d_{23}\mathrm{Re}\rho_{23}(z,t), \quad (8)$$

$$\frac{\partial^2 E(z,t)}{\partial z^2} - \frac{1}{c^2}\,\frac{\partial^2 E(z,t)}{\partial t^2} = \frac{4\pi}{c^2}\,\frac{\partial^2 P(z,t)}{\partial t^2}. \quad (9)$$

Here d_{12}, d_{13}, d_{23} are the matrix elements of the dipole moments of the transitions, T_{ik} are the relaxation times. The parameter values are chosen for atomic hydrogen and are given in the table [21]. Relaxation times in gases lie in the nanosecond range, which is much longer than the time intervals considered below (femtoseconds). The pulses interact with the medium coherently, their lengths and intervals between them are shorter than the relaxation times, which are insignificant in this case. The one-dimensional wave equation describes the propagation of sub-cycle pulses in near-field or coaxial waveguides [13]. The observation of DM in real media requires media with large values of polarization relaxation time T_2 which is easily realized in gases, nanoscale structures at low temperatures.

The initial conditions were chosen as follows. 2 pulses were launched into the vacuum from the left, point $z = 0$, and right ends of the integration regions, point $z = L$ ($L = 12\lambda_0$ is the length of the integration region, λ_0 is the wavelength of the main transition). The first is a rectangular pulse, in the form of a hypergaussian function:

$$E(z=0,t) = E_{01}e^{-\frac{(t-\Delta_1)^{20}}{\tau^{20}}}. \quad (10)$$

The second semi-cyclic pulse moved towards the first one and had a Gaussian shape:

$$E(z=L,t) = E_{02}e^{-\frac{(t-\Delta_2)^{2}}{\tau^{2}}}. \quad (11)$$

The medium was placed between points with coordinates from $z_1 = 2\lambda_0$ to $z_2 = 10\lambda_0$. The collision of pulses occurred at the point $z = z_{col} = 6\lambda_0$. Ideal mirrors were placed on the boundaries of the integration region. When reflected from them, the pulses entered the medium again and collided in it.

Symmetrical collision between pulses

The first example considers the case of the so-called symmetric collision of pulses in the medium, when the pulses simultaneously entered the medium and collided at its center. This is achieved by equalizing the delays $\Delta_1 = \Delta_2 = 2.5\tau$. The results of numerical simulations of the spatial and temporal dynamics of the medium polarization and population difference at the three resonant transitions are shown in Fig. 1–4. The parameters are listed in the table.

The collisions occur sequentially at times $t_{c1} = 2.7$ fs, $t_{c2} = 7.6$ fs, $t_{c3} = 12.6$ fs, etc. fs. As can be seen from

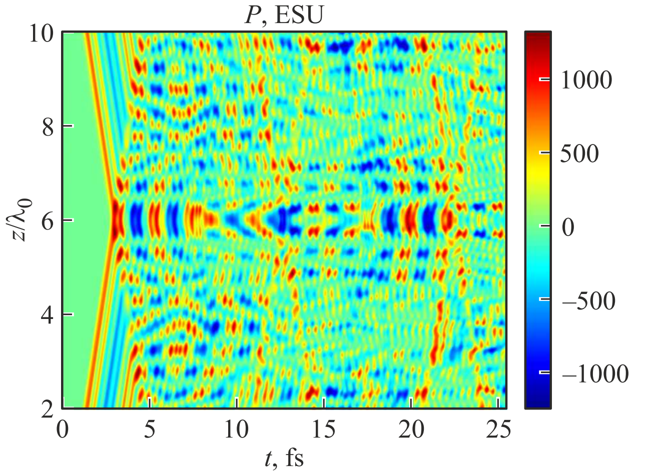

Figure 1. Spatial and temporal dynamics of polarization of a three-level medium $P(z, t)$.

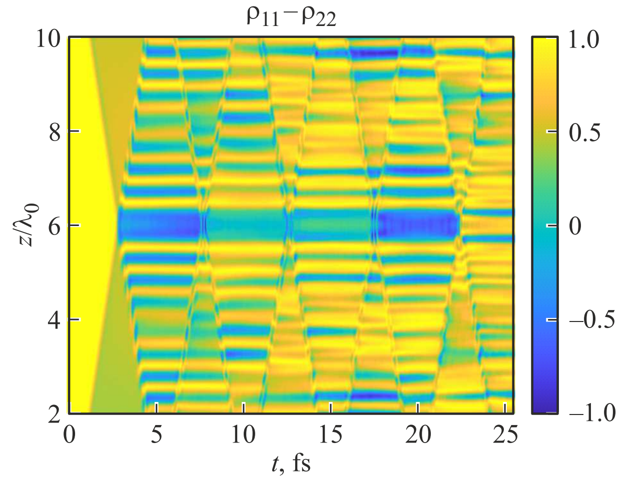

Figure 2. Spatial and temporal dynamics of the population difference $\rho_{11} - \rho_{22}$ of a three-level environment.

Fig. 2–4, a rather broad region with an almost constant value of the population difference appears in the pulse overlap region near the point $z = z_{col} = 6\lambda_0$. Bragg lattices of atomic populations arise to the left and right of it. After each collision, the shape of these lattices and the value of the inversion at the center change. This is due to the change in the character of polarization fluctuations (coherence of the medium) after each collision. It is the interaction of incident pulses with medium coherence fluctuations that is the physical mechanism for the formation of Bragg lattices of atomic populations at each medium transition, see [22] and [16–18] for more details.

The changes in the shape of the resonators after each collision indicate the dynamical nature of the induced structures, distinguishing them from conventional microresonators. This behavior of DM is analogous to the case when pulses of the same (Gaussian shape) and small amplitude collided in a two-level medium [18]. Differences are obviously to be expected at stronger fields, such as when the pulses act like self-induced transparency (SIT) pulses, which is beyond the scope of this paper.

Nonsymmetric momentum collision

In the example of the so-called symmetric collision of pulses, they entered the medium simultaneously and collided in its center. By varying the delays between them, it is possible to consider the situation when the pulses enter the medium non-simultaneously and collide in it off-center (the case of „unsymmetric“ collision). The delay is $\Delta_2 = 7.5\tau$ in the following example. The other parameters are as in Fig. 1–4. The results of numerical calculations showing the dynamics of the population difference at all transitions of the medium are shown in Fig. 5–7. The first collision of pulses at the given parameters occurs at the point $z_c = 7.3\lambda_0$ at time

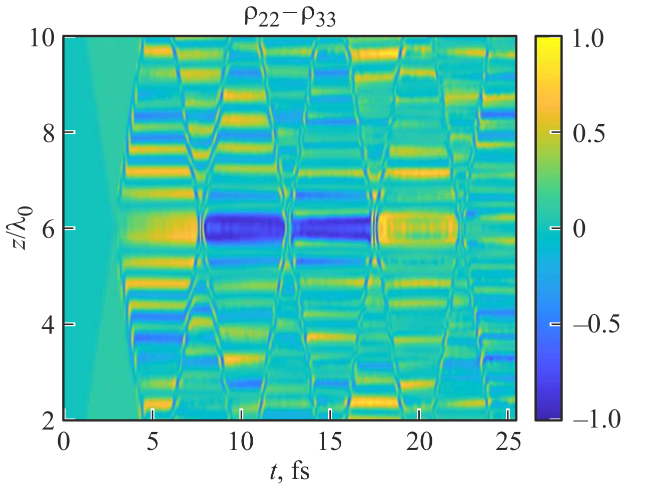

Figure 3. Spatial and temporal dynamics of the population difference $\rho_{22} - \rho_{33}$ of a three-level environment.

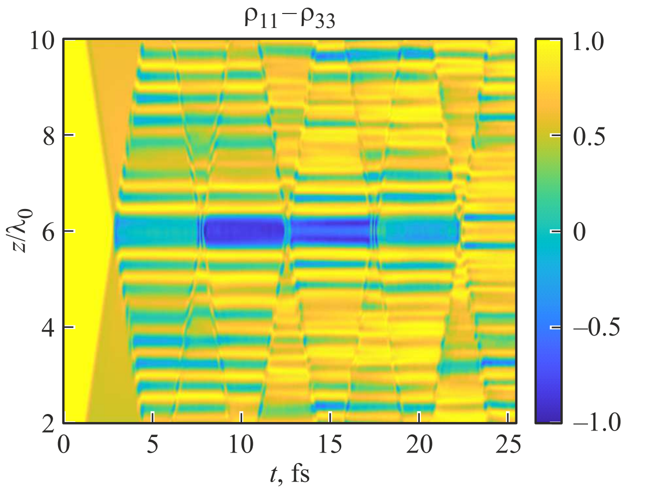

Figure 4. Spatial and temporal dynamics of the population difference $\rho_{11} - \rho_{33}$ of a three-level environment.

Parameters used in numerical calculations

Frequency (wavelength λ_0) $1 \to 2$	$\omega_{12} = 1.55 \cdot 10^{16}$ rad/s ($\lambda_{12} = \lambda_0 = 121.6\,nm$)
Dipole moment of transition $1 \to 2$	$d_{12} = 3.27\,\mathrm{D}$
Frequency (wavelength) of transition $1 \to 3$	$\omega_{13} = 1.84 \cdot 10^{16}$ rad/s ($\lambda_{13} = 102.6\,\mathrm{nm}$)
Dipole moment of the transition $1 \to 3$	$d_{13} = 1.31\,\mathrm{D}$
Frequency (wavelength) of transition $2 \to 3$	$\omega_{23} = 2.87 \cdot 10^{15}$ rad/s ($\lambda_{23} = 656.6\,\mathrm{nm}$)
Dipole moment of the transition $2 \to 3$	$d_{23} = 12.6\,\mathrm{D}$
Concentration of atoms	$N_0 = 2 \cdot 10^{20}\,\mathrm{cm}^{-3}$
Field amplitude	$E_{01} = 840000$ ESU $E_{02} = 1008000$ ESU
Parameter τ	$\tau = 200$ as
Delays $\Delta_1 = \Delta_2$	$\Delta_1 = \Delta_2 = 2.5\tau$

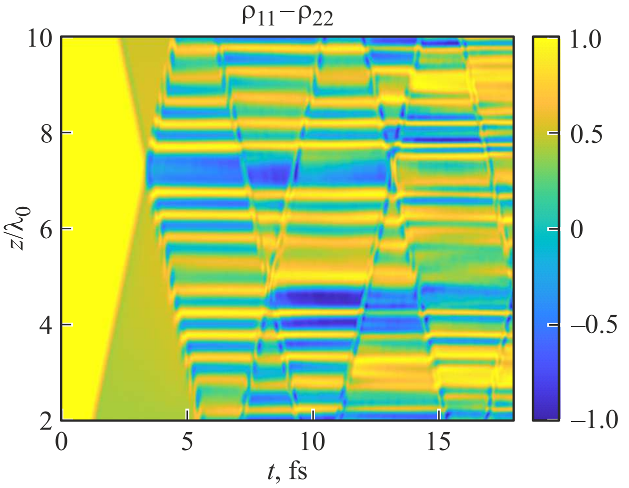

Figure 5. Spatial and temporal dynamics of the population difference $\rho_{11} - \rho_{22}$ of a three-level medium.

$t_c = 3.44$ fs. The second collision of pulses occurred at $z_c = 8.3\lambda_0$ and at time $t_c = 4.8$ fs, etc. Each subsequent collision occurred at different time moments due to the delay.

The DMs appeared at different moments of time in different regions of the medium as a result of such asymmetric„collision“The parameters of the induced Bragg gratings (shape, number of periods, etc.) could differ to the left and right of the pulse overlap region due to the asymmetry of the problem. The use of asymmetric collisions opens up additional possibilities in controlling the shape of induced structures, as previously noted in Ref. [23], in which an asymmetric collision of rectangular SIT pulses was considered.

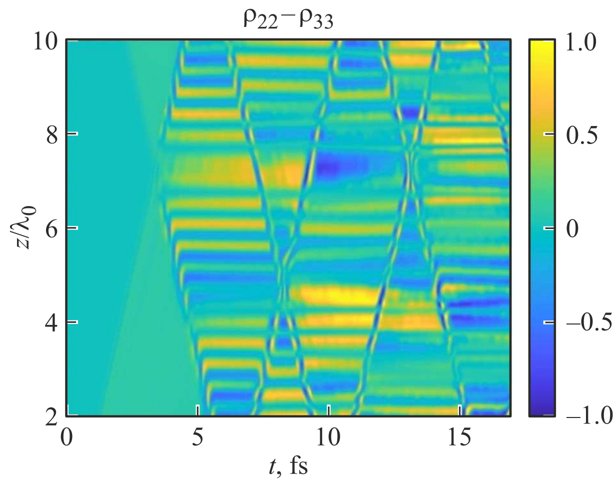

Figure 6. Spatial and temporal dynamics of the population difference $\rho_{22} - \rho_{33}$ of a three-level environment.

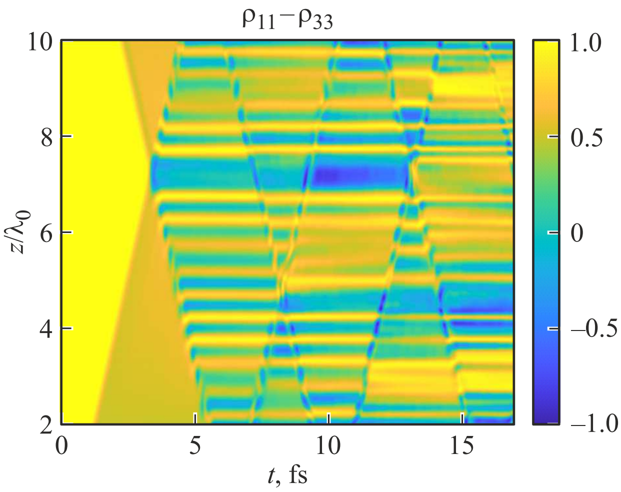

Figure 7. Spatial and temporal dynamics of the population difference $\rho_{11} - \rho_{33}$ of a three-level environment.

Conclusion

The dynamics of DM in case of collisions of unipolar light pulses with different profiles — rectangular and Gaussian — was studied in this paper in a three-level medium under weak excitation conditions, based on numerical simulations. The case of symmetric collision of pulses, when the pulses simultaneously entered the medium and collided in its center, was considered. In this case, due to the rectangular profile of one of the pulses, the population difference maintained a constant value at the center of the medium, while periodic population Bragg gratings formed at the edges. This case is qualitatively similar to the previously studied case of collision of semi-cyclic pulses of the same shape (Gaussian shape) with small amplitude and in a two-level medium. In the case of asymmetric collision of pulses due to the delay between them, DMs appeared in different regions of the medium and the shape of Bragg gratings also looked different to the left and right of the region of pulse overlap. This makes it possible to create DMs of asymmetric shape with different parameters of Bragg mirrors lying to the left and right of the overlap region.

The obtained results demonstrate the possibility of realizing media parameters of which change in space and time in ordinary atomic media under the action of extremely short pulses. Any media with a large value of phase memory time T_2 can be used to realize such media under these conditions, and it is not necessary to use the various artificial media and metamaterials that are currently specially developed for the practical realization of time-dependent media [9–11,24,25].

Funding

The study was financially supported by RNF under the scientific project 23-12-00012 (numerical modeling of symmetric collision between pulses) and under the State assignment of Ioffe Institute of Physics and Technology, topic 0040-2019-0017 (numerical modeling of asymmetric collision between pulses).

Conflict of interest

The authors declare that they have no conflict of interest.

References

[1] K.J. Vahala. Nature, **424**, 839 (2003).
[2] H. Cao, J. Wiersig. Rev. Mod. Phys. **87**, 61 (2015).
[3] A. Pasquazi, M. Peccianti, L. Razzari, D.J. Moss, S. Coen, M. Erkintalo, Y.K. Chembo, T. Hansso et al. Phys. Rep., **729**, 1−81 (2018).
[4] Y. Sun, J. Wu, M. Tan, X. Xu, Y. Li, R. Morandotti, A. Mitchell, D.J. Moss. Adv. Opt. Photon., **15** (1), 86−175 (2023).
[5] E.A. Anashkina, M. P. Marisova, A. N. Osipov, A.V. Yulin, A.V. Andrianov. IEEE J. Sel. Top. Quantum. Electron., **30** (5), Art no. 2900208 (2024).
[6] L. Zhang, J. Hu, J. Wu, R. Su, Z. Chen, Q. Xiong, H. Deng. Progress in Quantum Electron., **83**, 100399 (2022).
[7] J.P. Reithmaier, G. Sęk, A. Löffler, C. Hofmann, S. Kuhn, S. Reitzenstein, L.V. Keldysh, V.D. Kulakovskii, T.L. Reinecke, A. Forchel. Nature, **432**, 197−200550 (2004).
[8] H. Yu, X. Liu, W. Sun, Y. Xu, X. Liu, Y. Liu. Opt. & Laser Technol., **177**, 111099 (2024).
[9] T.T. Koutserimpas, F. Monticone. Opt. Mater. Express., **14**, 1222−1236712 (2024).
[10] Y. Sharabi, A. Dikopoltsev, E. Lustig, Y. Lumer, M. Segev. Optica, **9** (6), 585 (2022).
[11] K. Pang, M.Z. Alam, Y. Zhou, C. Liu, O. Reshef, K. Manukyan, M. Voegtle, A. Pennathur, C. Tseng, X. Su, H. Song, Z. Zhao, R. Zhang, H. Song, N. Hu, A. Almaiman, J.M. Dawlaty, R.W. Boyd, M. Tur, A.E. Willner. Nano Lett., **21** (14), 5907 (2021).
[12] F. Krausz. Reviews of Modern Physics, **96**, 030502 (2024).
[13] N.N. Rosanov, M.V. Arkhipov, R.M. Arkhipov, A.V. Pakhomov. Contemporary Physics, **64** (3), 224 (2023).
[14] N.N. Rosanov, M.V. Arkhipov, R.M. Arkhipov. Phys. Usp. **67** (11), 1129 (2024). DOI: 10.3367/UFNe.2024.07.039718.
[15] N.N. Rozanov, M.V. Arhipov, R.M. Arhipov. Teragertsovaya fotonika, pod red. V.Ya. Panchenko, A.P. Shkurinov (RAS, M., 2023), p. 360−393 (in Russian).
[16] O.O. Diachkova, R.M. Arkhipov, M.V. Arkhipov, A.V. Pakhomov, N.N. Rosanov. Opt. Commun., **538**, 129475 (2023).
[17] O. Diachkova, R. Arkhipov, A. Pakhomov, N. Rosanov. Opt. Commun., **565**, 130666 (2024).
[18] R. Arkhipov, A. Pakhomov, O. Diachkova, M. Arkhipov, N. Rosanov. JOSA B, **41** (8), 1721 (2024).
[19] R.M. Arkhipov, O.O. D'yachkova, M.V. Arkhipov, A.V. Pakhomov, N.N. Rosanov. Opt. i spektr., **132** (9), 919 (2024) (in Russian).
[20] A. Yariv. Quantum Electronics (John Wiley & Sons, N.Y., London, Toronto, 1975).
[21] S.E. Frisch. *Optical spectra of atoms* (State Publishing House of Physical and Mathematical Literature, Moscow-Leningrad, 1963).
[22] R.M. Arkhipov. JETP Lett., *113*, 611 (2021).
[23] R.M. Arkhipov, O.O. D'yachkova, M.V. Arkhipov, A.V. Pakhomov, N.N. Rosanov. Opt. i spektr., **133** (2), 184 (2025) (in Russian).
[24] N. Engheta. Nanophotonics, **10** (1), 639−642 (2020).
[25] V. Pacheco-Peña, D. M. Solís, N. Engheta. Opt. Mater. Express, **12** (10), 3829−3836 (2022).

Translated by A.Akhtyamov